DOI https: //doi. org/10.1007/s11595-020-2283-8

Effect of Adding Microwave Absorber on Structures and Properties of Hypercoal-Based Activated Carbons

XU Lijun[1], FAN Lihua[1,2*], HOU Caixia[1,2], LIU Junke[1], SUN Zhang[1,2]

(1.College of Chemical Engineering, North China University of Science and Technology, Tangshan 063210, China; 2.Hebei Province Key Laboratory of Photocatalytic and Electrocatalytic Materials for Environment, Tangshan 063210, China)

Abstract: Using lignite-based hypercoal as raw material, KOH as activator and CuO as microwave absorber, we prepared hypercoal-based activated carbons by microwave-assisted activation. The pore structure and the electrochemical performance of the activated carbons were tested, and the effects of adding CuO in the activation reaction process were also investigated. The activated carbons prepared were characterized by nitrogen adsorption-desorption, X-ray diffraction (XRD) and scanning electron microscopy (SEM). The specific surface area and mesoporous ratio of the hypercoal-based activated carbon are 1 257 m^2/g and 55.4%, respectively. When the activated carbons are used as the electrode materials, the specific capacitance reaches 309 F/g in 3 M KOH electrolyte. In comparison with those prepared without CuO absorber, the specific capacitance increases by 11.6%. It was proved that the addition of microwave absorber in microwave-assisted activation was a low-cost method for rapidly preparing activated carbon, and it could effectively promote the development of the pore structure and improve its electrochemical performance.

Key words: hypercoal; activated carbon; microwave absorber; pore structure; electrochemical performance

1 Introduction

With the consumption of the resource increasing sharply, the green and renewable development mode has gradually become the mainstream of social development. Electric double layer capacitor (EDLC) has attracted the extensive attention of researchers because of its high power density and long cycle life. With the efforts of researchers, great progress has been made in the study of electrode materials for EDLC. The application of new materials such as carbon nanotube and graphene has greatly promoted the development of electrode materials. However, at present, activated carbon with highly developed pore structure and rich functional groups is still the first choice for EDLC electrode materials, and it has unparalleled advantages in industrial production[1,2]. In China, using coal as precursor to prepare activated carbon has great raw material advantage, especially. The hypercoal is the coal which has been deashed by high-temperature solvent extraction. The activated carbon prepared by hypercoal has a lot of advantages such as less impurities and abundant functional groups[3,4].

The traditional activated carbon preparation process requires long time (usually 1-2 h). In order to increase the production efficiency, a lot of researchers begin to use microwave heating technology to produce activated carbon. Microwave heating raises the temperature of heated object by causing the dipolemolecules inside the material to reciprocate at a high frequency to generate "internal friction heat" [5,6]. The preparation of activated carbon by microwave heating technology can not only improve the production efficiency, but also make the properties of activated carbon more uniform. Xing[7] prepared activated carbon with a specific surface area of 3 064 m^2/g in the microwave reactor in only 20 min, indicating that microwave heating is a high efficient activation method. Zhang[8] also obtained the similar conclusions when using microwave heating to prepare activated carbon. The activated carbons with specific surface area of 1 079-1 536 m^2/g were prepared within only 2-10 min.

(Received: Apr. 15, 2019; Accepted: Feb. 18, 2020)

XUN Lijun(许立军): E-mail:2488852681@qq.com

*Corresponding author: FAN Lihua(樊丽华): Prof.; Ph D; E-mail: lihuafan71@126.com

Funded by the National Natural Science Foundation of China (No.51874136), Natural Science Foundation of Hebei Province (No. B2017209240)

Since coal has a low dielectric constant (between 4.7 and 5.3), its temperature rise in the microwave field usually requires the aid of microwave absorbers[9-11]. Monsef-Mirzai[12] studied the effects of three kinds of microwave absorbers on the pyrolysis process of coal. It was found that the addition of microwave absorber changed the pyrolysis efficiency of coal, indicating that the microwave absorber could affect the pyrolysis of coal by changing the heating process of coal. The preparation of coal-based activated carbon is a composite process composed of coal pyrolysis and reaction between coal and activator. In theory, in the process of preparing activated carbon by microwave heating, the addition of microwave absorber can affect the properties of activated carbon by changing the pyrolysis process of coal. After adding microwave absorber, the increase of the heating rate will also raise the reaction extent between coal and activator, which can promote the development of the pore structure of activated carbon and enhance its performance. Therefore, it is an available method to optimize and modify the properties of activated carbon by adding microwave absorber. However, there is little information available about the influence of microwave absorber on the activated carbon.

The main purpose of the present study is to use hypercoal as raw materials, KOH as activated agent and CuO as microwave absorber to develop a microwave -assisted activation process for the preparation of activated carbon for EDLC electrode materials. The pore structure, microcrystal structure and electrochemical performance of the activated carbons were investigated in detail. In contrast to the activated carbon prepared without CuO absorber, the improvement of adding CuO on activated carbon properties and preparation process were also discussed.

2 Experimental

2.1 Materials and reagents

The properties of the raw materials were shown in Table 1. The hypercoal was extracted from Mongolian lignite (D<0.075 mm) by N-methylpyrrolidone in a high pressure reactor.

2.2 Preparation of activated carbon

The hypercoal and KOH were uniformly mixed in deionized water at a mass ratio of 1.5:1. After drying, the mixture was transferred into a microwave reactor. The microwave power was adjusted to 2 000 W, and the temperature was raised to 600 ℃ and kept for 6 min in N_2 atmosphere. After cooling to room temperature, the residue was washed with HNO_3(0.5%) and rinsed with deionized water until the pH of the waste solution was about 6-7, and then dried at 120 ℃ for 2 h. The activated carbon was tagged as HAC-mic. Under the same preparation conditions, CuO was mixed with KOH and hypercoal with a mass ratio of C:Cu=100:1.5, and then activated it. After the temperature was declined to room temperature, some of the activated materials were treated with HNO_3 for removing Cu-impurity and washed with deionized water until the pH of the waste solution was 6-7. The final products were dried at 120 ℃ for 2 h, and were tagged HAC-CuO. The remaining activated materials were directly rinsed with deionized water and then dried at 120 ℃ for 2 h, which were tagged HAC-CuO-R.

The activated carbon, polytetrafluoroethylene and acetylene black were mixed, and then pressed onto a nickel foam current collector at 10 MPa to form an electrode. After drying at 120 ℃ for 2 h, two electrodes were assembled into an EDLC together with 3 M KOH electrolyte and a polypropylene septum.

2.3 Porosity and capacitance measurement

The N_2 adsorption-desorption isotherms of activated carbons were obtained at 77 K with the aid of a surface area and pore size analyzer (Beishide, 3H-2000PM1, Beijing, China). The specific surface area was calculated by BET model. The micropore distribution was calculated by DFT model, and the mesopore distribution was calculated by BJH model. The micropore volume was calculated by T-plot method, and the mesopore volume was obtained by

Table 1 Proximate, ultimate and mineral composition analyses of raw materials

Sample	Proximate analysis/wt%			Ultimate analysis/wt%				
	M_{ad}	V_{daf}	A_{ad}	C_{daf}	H_{daf}	O*	N_{daf}	S_{daf}
Lignite	11.06	47.81	9.65	61.90	4.20	32.81	0.77	0.32
Hypercoal	1.07	64.07	0.09	79.74	6.45	9.59	3.96	0.25
	Mineral composition/wt%							
	Al_2O_3	SiO_2	Na_2O	K_2O	CaO	Fe_2O_3	MgO	
Lignite	0.842 1	1.634 5	0.298 8	0.021 5	2.976 4	0.311 2	0.321 1	

record: ad-air dried basis; daf-dry ash-free basis; *- minusing

subtracting the micropore volume from the total pore volume. The morphology of the activated carbon microscopic pore structure was observed by scanning electron microscopy (SEM, JSM-IT100, Japan). Microcrystal structure patterns of activated carbon were measured by X-ray diffraction (XRD, D/MAX2500PC, Japan), using a Cu Kα radiation at 40 kV and 40 mA as the X-ray source. The lateral size L_a and the stacking height L_c of the graphite crystallite were determined from Scherrer Eq: $L_a=1.84\lambda/(\beta_{100}\cdot\cos\theta_{100})$ and $L_c=0.94\lambda/(\beta_{002}\cdot\cos\theta_{002})$, where λ was the wavelength of the radiation used, β_{100} and β_{002} were the widths of the (100) and (002) peaks, respectively. The interlayer spacing (d_{002}) within aromatic layer was determined using Bragg Eq: $d_{002}=\lambda/2\sin\theta_{002}$ [13].

Cyclic voltammetry and electrochemical impedance spectroscopy were carried out by an electrochemical workstation (CHI660D, Shanghai Chenhua, China) at room temperature. Galvanostatic discharge-charge test was performed using a battery detection system (CT2001A, Wuhan LANHE, China) over the range of 0.05-0.9 V. The specific capacitance of the activated carbon electrode was calculated based on charge -discharge cycles according to the Eq: $C_g=2I\Delta t/m\Delta V$, where C_g was the specific gravimetric capacitance (F/g), I was the discharge current (A), Δt was the discharge time (s), ΔV was the discharge voltage (V), and m represented the mass (g) of the active materials in a single electrode[14].

3 Results and discussion

3.1 Activated carbon properties

Fig.1 shows the N_2 adsorption-desorption isotherms of the activated carbon samples. Isotherms of all samples correspond to the type I adsorption isotherms, which exhibit a large adsorption capacity in the low pressure range. There is an apparent hysteresis loop when P/P_0 is over 0.4, which indicates the coexistence of well-developed micropores and a considerable amount of mesopores[15]. It is found that the adsorption capacity of HAC-mic and HAC-CuO-R is similar. After removing the Cu-impurity, the adsorption capacity of HAC-CuO is significantly higher than those of the other two activated carbon samples, which is attributed to pore blockage resulting from the Cu-impurity. The participation of CuO in the activation reaction is beneficial to the further development of the pore structure of activated carbon.

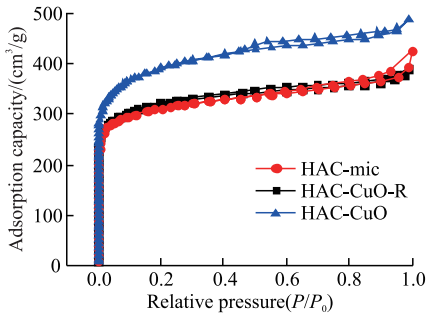

Fig.1 N_2 adsorption-desorption isotherms of activated carbons

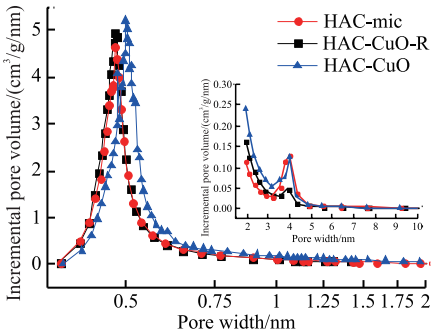

Fig.2 Pore distribution of activated carbons

The pore distribution of activated carbons is shown in Fig.2. It can be seen that the micropore distribution of the three samples is concentrated between 0.4-0.8 nm. A large number of micropore of HAC-mic and HAC-CuO-R are distributed around 0.4 nm. However, the most micropore of HAC-CuO are distributed around 0.5 nm. It is obvious that the micropore sizes will increase with the addition of CuO to participate in the activation reaction. As listed in Table 2, the specific surface area and mesoporous ratio of HAC-mic are only 1 035 m^2/g and 38%, respectively. But the specific surface area and mesoporous ratio of HAC-CuO increase to 1 257 m^2/g and 55.4%. It can be confirmed that CuO can not only enlarge the micropores size, but also optimize the pore structure of activated carbons.

Many researchers believed that the micropores

Table 2 Pore structure parameters of activated carbons

Sample	S_{BET}/(m^2/g)	V_{tol}/(cm^3/g)	V_{mic}/(cm^3/g)	V_{mes}/(cm^3/g)	V_{mes}/V_{tol}/%
HAC-mic	1 035	0.71	0.44	0.27	38.0
HAC-CuO-R	1 017	0.60	0.32	0.28	46.7
HAC-CuO	1 257	0.74	0.33	0.41	55.4

S_{BET}-BET specific surface area; V_{tol}-total pore volune; V_{mic}-micropore volume; V_{mes}-mesopore volume; V_{mes}/V_{tol}-mesoporous ratio

whose sizes are 2 to 4 times of the adsorbed ions and larger than 0.5 nm are more favorable to adsorbing electrolyte to form electric double layer[16,17]. The ionic diameter of K^+ is about 0.26 nm, and it can be seen that HAC-CuO is more suited to the requirements for EDLC electrode materials.

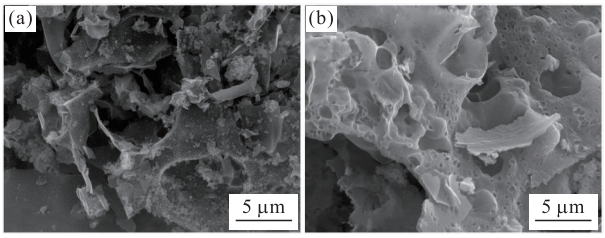

Fig.3 Representative SEM images of activated carbons: (a) HAC-CuO-R; (b) HAC-CuO

Fig.3 shows the representative SEM image of HAC-CuO-R and HAC-CuO. It can be seen that there are some flocs on the surface of HAC-CuO-R and some pores are blocked by the flocs. However, when the Cu-impurity is removed, the flocs disappear and the surface of HAC-CuO becomes smooth and cleaned. This phenomenon confirms that Cu-impurity will make the pores blocked.

In order to determine the ingredients of Cu-impurity, HAC-mic, HAC-CuO-R and HAC-CuO were tested by XRD. XRD pattern of HAC-CuO-R is shown in Fig.4(a). By comparing to the standard cards, it can be found that HAC-CuO-R has the diffraction peaks corresponding to Cu in the vicinity of 2θ=43.3°, 50.4°, and 74.1°, indicating that CuO is reduced to Cu during the activation reaction[18]. At high temperature, CuO could cause "sparking phenomenon" in the microwave field[19], which would promote the temperature to rise rapidly and accelerate the reaction with C.

The broad peak at 2θ=15°-30° shown in XRD patterns of HAC-mic and HAC-CuO was divided into 002 peaks representing aromatic carbon and γ peaks representing aliphatic carbon[20-22]. f_a is the ratio of aromatic carbon atoms to total carbon atoms in a coal molecular structural unit, which can be defined as $f_a=C_{ar}/(C_{ar}+C_{al})$. The schematic illustration of curve-fitted XRD pattern is shown in Fig.4(b). The corresponding microcrystal structure parameters of the activated carbon are shown in Table 3.

Table 3 Microcrystal structure parameters of activated carbons

Samples	L_a/nm	L_c/nm	d_{002}/nm	f_a
HAC-mic	3.511	0.825	0.344	0.76
HAC-CuO	3.391	0.854	0.348	0.81

It can be seen from Table 3 that HAC-mic and HAC-CuO have no obvious difference in L_c and d_{002}, but HAC-CuO has a smaller L_a than HAC-mic, which reflects that the graphite crystallites of HAC-CuO are finer and smaller. Kaneko[23] showed that the disordered arrangement of graphite crystallite constitutes the micropores of activated carbon. Finer and smaller graphite crystallite could increase the number of micropores and form larger specific surface area. At the same time, the f_a of HAC-CuO was slightly larger than that of HAC-mic, indicating that more surface functional groups and aliphatic chains react with the activator. So it is obvious that the addition of CuO could not only promote the splitting of the aromatic structure during the activation process, but also cause a larger amount of non-aromatic structure to lose.

3.2 Discussion on activation mechanism

In the process of preparing activated carbon by microwave-assisted heating, since hypercoal can hardly absorb microwave, KOH will heat the hypercoal in the initial stage of activation reaction. After hypercoal is heated to a certain temperature, KOH begins to react with the functional groups and aliphatic chains of hypercoal to cause a loss of non-aromatic structure, which releases the space between the graphite crystallites to form the initial micropores. At the same time, some defects will be caused on aromatic ring by these reactions. The defects will be used as active sites that can easily cause distortion and breakage of the aromatic layers due to the high reactivity of active

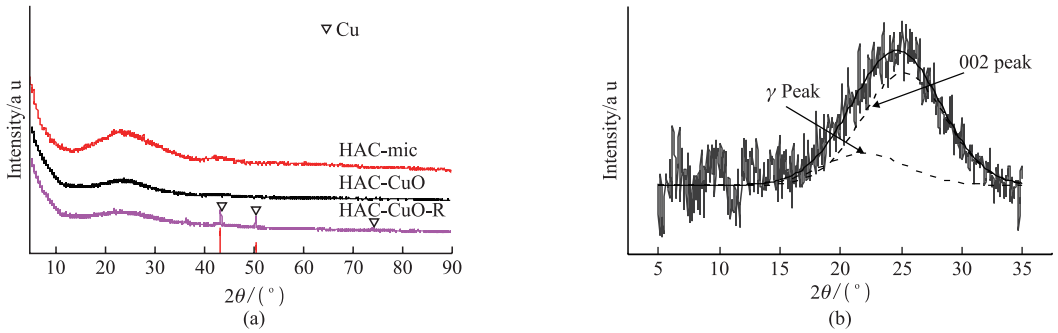

Fig.4 XRD patterns of activated carbons: (a) XRD patterns; (b) Schematic illustration of curve-fitted XRD pattern of 002 peak and γ peak

sites. These changes of crystallite structure contribute to the formation of micropores. As the activation temperature increases, there are many pores generated inside the hypercoal. The porous carbon with good dielectric properties[24,25] can absorb the microwave intensely and make itself to be heated, causing the temperature of the pore wall to be higher than that of the unactivated hypercoal, thereby making the activator more prone to react with the pore wall. The activator would gradually convert from KOH to K_2CO_3[26] at high temperature. K_2CO_3 can catalyze the ring opening of the aromatic structure by generating CO^-K^+ complex[27], so that the pore walls composed of graphite crystallites become thinner, resulting in a pore-expanding effect. Therefore, more active sites are generated in the initial stage of the reaction, and larger space are released by the non-aromatic structure loss, resulting in more pores formed[28].

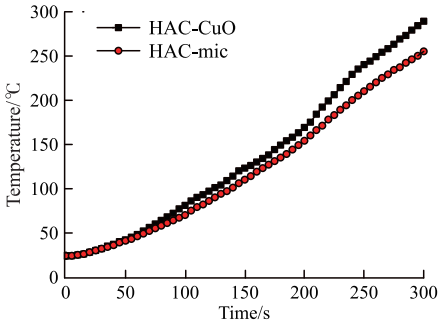

Fig.5 Temperature rise condition of HAC-CuO and HAC-mic in the initial stages of activation

CuO plays two roles in the activation reaction. Firstly, CuO can heat hypercoal. CuO has faster rate of temperature rise than KOH in the microwave field because it is a strong microwave absorbing material with a large dielectric constant. CuO is heated up quickly in the initial stage of the reaction and transfers energy to adjacent hypercoal molecules, reducing the time of heat transfer between the activator and hypercoal. So the activation reaction is accelerated, and more micropores are generated. The temperature changes of HAC-CuO and HAC-mic within the first 5 min of the activation process are shown in Fig.5. It is obvious that the heating rate of HAC-CuO is higher than that of HAC-mic, which indicates that the materials with CuO can more fully react with KOH at the low temperature stage. More non-aromatic structure such as functional groups and aliphatic chains will react with the activator, leading to larger f_a of HAC-CuO than that of HAC-mic. Larger space between the graphite crystallites is cleaned and form pores. During the reaction of hypercoal with KOH, more active sites are left on the aromatic structure of hypercoal[29]. Active sites are able to cause the aromatic layers to be more severely damaged by further reaction, making the graphite crystallites become more distorted. These changes lead to higher specific surface area and larger total pore volume of HAC-CuO, and its pore structure is more suitable for EDLC electrodes. Fig.6 is the schematic diagram of activated carbon activation process. The A process represents the activation of HAC-mic and the B process represents the activation of HAC-CuO. The main difference between the two processes is that the B process produces more initial micropores than those in the A process.

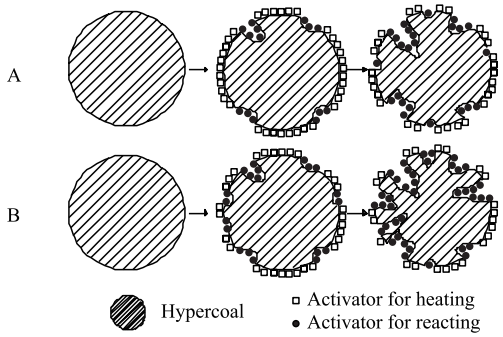

Fig.6 Schematic of the different activated processes

Secondly, when the reaction temperature is high, CuO will also react with the adjacent porous carbon directly to further consume C atoms, which is favorable for the pore expansion. It can be seen from Fig.6 that a large number of micropores of HAC-CuO are expanded into mesopores, making the mesoporous ratio of HAC-CuO reach 55.4%. In summary, CuO can promote the development of pore structure of activated carbon.

3.3 Electrochemical performance test

Fig.7 shows the electrochemical performances of activated carbon electrodes in 3 M KOH electrolyte. Nyquist plots of activated carbon are displayed in Fig.7(a). The Nyquist plots can not only test the equivalent series resistance of EDLC, but also reflect the pore structural characteristics of the electrode materials. As HAC-CuO has developed pore structures and smaller graphite crystallites, the transfer of electrons between activated carbon particles becomes more difficult. This leads to that HAC-CuO electrode exhibits bigger semicircle at high frequency region, reflecting higher interfacial charge transfer resistance. But in the middle frequency region, HAC-CuO electrode has shorter straight line with a slope of 45°, suggesting lower ion diffusion resistance[30]. All the activated carbon samples display a straight line nearly vertical to real axis in the impedance plot in the low frequency region, especially for HAC-CuO, demonstrating an ideal capacitor behavior.

Fig.7(b) presents the cyclic voltammetry curves

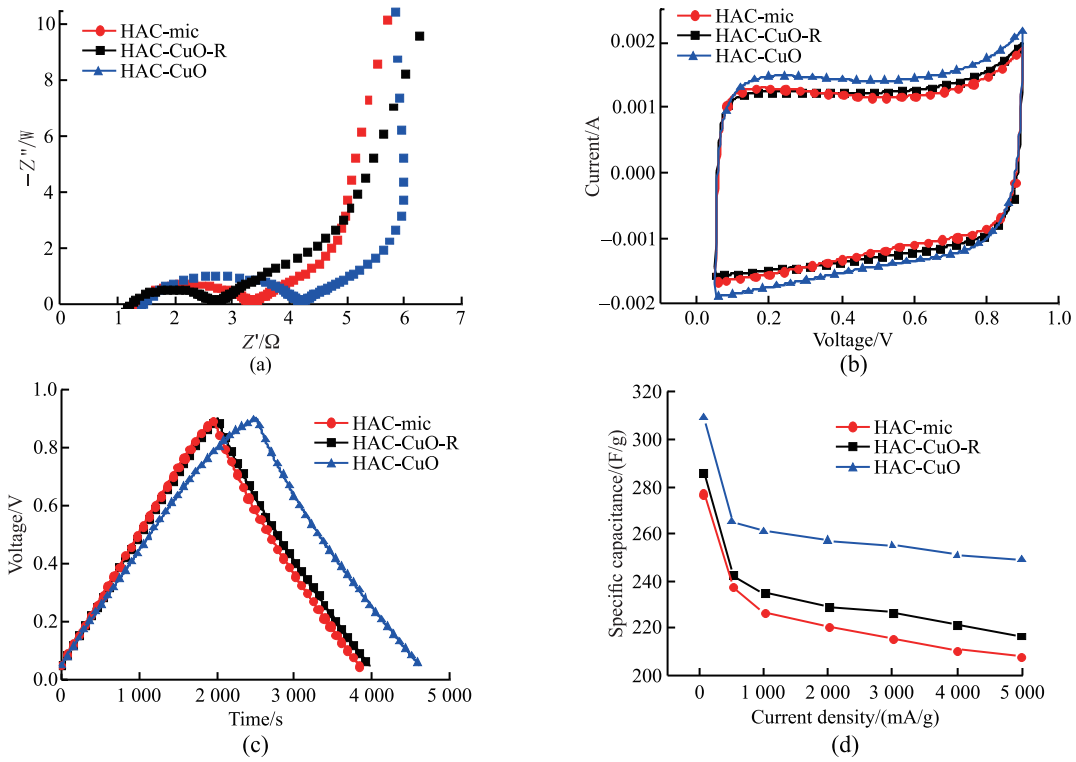

Fig.7 Electrochemical performances of the activated carbon electrodes in 3 M KOH electrolyte: (a) Nyquist plots, (b) cyclic voltammetry, (c) Galvanostatic charge-discharge curves, (d) Gravimetric capacitance against current density

of the activated carbon electrodes. In the range of 0.05-0.9 V, the curves exhibit a rectangular-like shape without obvious redox-peaks appearing, indicating that EDLC relies on forming an electric double layer at the phase interface to store energy[31]. HAC-CuO and HAC-CuO-R have less non-aromatic structure, and almost no chemical reaction occurs between the electrode materials and electrolyte during charging and discharging, so the cyclic voltammetry curves of HAC-CuO and HAC-CuO-R are closer to desirable rectangle. Although HAC-CuO-R contains Cu, Cu does not react with KOH aqueous electrolyte to produce additional pseudo-capacitance. The area enclosed by the rectangular curve can reflect the amount of specific capacitance, as can be seen from Fig. 7(b), and the specific capacitance of HAC-CuO electrode is the largest.

Fig.7(c) shows the galvanostatic discharge-charge curves of activated carbons at current density of 50 mA/g. All the samples exhibit highly symmetric triangular test curves, suggesting a typical capacitive behavior and superior electrochemical reversibility at the loading current. The three activated carbon electrodes have no ohmic drop at the beginning of the discharge process, indicating that the internal resistances of all the EDLCs are small[32,33]. It is apparent that HAC-CuO electrode shows the longest discharge time among the three samples under the same test condition, which attributes to high specific surface area and high mesoporous ratio, indicating that it has the highest specific capacitance. The corresponding specific capacitance of HAC-CuO reaches 309 F/g, which is higher than 277 F/g for HAC-mic and 285 F/g for HAC-CuO-R.

Fig.7(d) presents the relationship between the specific capacitance and current density of activated carbon electrodes. It mainly reflects the diffusing ability of the electrolyte in the electrode materials at different current densities, which is mainly related to the mesoporous ratio of the electrode material and the surface roughness of the pores[34]. Generally, higher mesoporous ratio of electrode materials provides higher specific capacitance retention rate. The specific capacitances of all the activated carbon samples decrease gradually with the increase of the current density, which is attributed to the limited transportation of the electrolyte ions in activated carbon pore structure during fast charging. When the current density increases to 5 000 mA/g, the specific capacitance of the HAC-CuO electrode decreases from 309 to 249 F/g, and the specific capacitance retention rate reaches 80.5%. Under the same test conditions, the specific capacitance retention rates of HAC-mic and HAC-CuO-R are only 75.1% and 75.7%, respectively. Although HAC-CuO-R has larger mesoporous ratio than HAC-mic, it

does not exhibit better specific capacitance retention rate because the Cu-impurity hinders the diffuse of the electrolyte.

4 Conclusions

Microwave-assisted activation process is a low-cost method for rapid preparation of activated carbon from hypercoal. In this process, CuO can help hypercoal heat up more quickly, so that make more hypercoal react with KOH to create micropores. After adding CuO, the specific surface area of activated carbon increases from 1 035 to 1 257 m^2/g, and the size of micropores has also been slightly enlarged. In the high temperature reaction stage, CuO directly participates in the pore-expanding reaction. The mesoporous ratio of activated carbon is increased from 38% to 55.4%. The specific surface area and the mesoporous ratio of activated carbon have been greatly increased. HAC-CuO electrode exhibits superior electrochemical performance such as high specific capacitance of 309 F/g and high specific capacitance retention rate of 80.5% at high current densities. Therefore, adding CuO during microwave-assisted activation is an effective method to improve the electrochemical performance of activated carbon electrode.

References

[1] Chen Y, Du L, Yang P, *et al*. Significantly Enhanced Robustness and Electrochemical Performance of Flexible Carbon Nanotube-Based Supercapacitors by Electrodepositing Polypyrrole[J]. *Journal of Power Sources*, 2015, 287: 68-74

[2] Das T, Chauhan H, Deka S, *et al*. Promising Carbon Nanosheet-Based Supercapacitor Electrode Materials from Low-Grade Coals[J]. *Microporous and Mesoporous Materials*, 2017, 253: 80-90

[3] Zhang Y, Yuan Z, Margni M, *et al.* Intensive Carbon Dioxide Emission of Coal Chemical Industry in China[J]. *Applied Energy*, 2019, 236: 540-550

[4] Dong Y, Jiang X, Ren M, *et al.* Environmental Implications of China's Wind-Coal Combined Power Generation System[J]. *Resources, Conservation and Recycling*, 2019, 142: 24-33

[5] Chandaliya V K, Biswas P P, Dash P S, *et al*. Producing Low-Ash Coal by Microwave and Ultrasonication Pretreatment Followed by Solvent Extraction of Coal[J]. *Fuel*, 2018, 212: 422-430

[6] Liew R K, Azwar E, Yek P N Y, *et al*. Microwave Pyrolysis with KOH/NaOH Mixture Activation: A New Approach to Produce Micro-mesoporous Activated Carbon for Textile Dye Adsorption[J]. *Bioresource Technology*, 2018, 266: 1-10

[7] Xing B, Huang G, Chen L, *et al.* Microwave Synthesis of Hierarchically Porous Activated Carbon from Lignite for High Performance Supercapacitors[J]. *Journal of Porous Materials*, 2016, 23(1): 67-73

[8] Zhang M Y, Zhao X, Zhuang Q C. Preparation and Electrochemical Properties of Multiscale Porous Active Carbon for Supercapacitor Electrodes Made from Ultra-Pure Lignite by Microwave Irradiation[J]. *International Journal of Electrochemical Science*, 2016, 11(3): 2 153-2 165

[9] Yagmur E, Simsek K E H, Aktas Z, *et al.* Effect of CuO Receptor on the Liquid Yield and Composition of Oils Derived from Liquefaction of Coals by Microwave Energy[J]. *Energy Conversion and Management*, 2008, 49(11): 3 043-3 050

[10] Samanli S. A Comparison of the Results Obtained from Grinding in a Stirred Media Mill Lignite Coal Samples Treated with Microwave and Untreated Samples[J]. *Fuel*, 2011, 90(2): 659-664

[11] Liu H P, Chen T P, Li Y, *et al*. Temperature Rise Characteristics of ZhunDong Coal During Microwave Pyrolysis[J]. *Fuel Processing Technology*, 2016, 148: 317-323

[12] Monsef-Mirzai P, Ravindran M, McWhinnie W R, *et al*. Rapid Microwave Pyrolysis of Coal: Methodology and Examination of the Residual and Volatile Phases[J]. *Fuel*, 1995, 74(1): 20-27

[13] Feng B, Bhatia S K, Barry J C. Structural Ordering of Coal Char During Heat Treatment and Its Impact on Reactivity[J]. *Carbon*, 2002, 40(4): 481-496

[14] Zhou Q, Gao J, Li C, *et al*. Composite Organogels of Graphene and Activated Carbon for Electrochemical Capacitors[J]. *Journal of Materials Chemistry A*, 2013, 1(32): 9 196-9 201

[15] Zhao X Y , Huang S S, Cao J P, *et al*. KOH Activation of a Hypercoal to Develop Activated Carbons for Electric Double-Layer Capacitors[J]. *Journal of Analytical & Applied Pyrolysis*, 2014, 105(5): 116-121

[16] Koresh J, Soffer A. Stereoselectivity in Ion Electroadsorption and in Double-Layer Charging of Molecular Sieve Carbon Electrodes[J]. *Journal of Electroanalytical Chemistry and Interfacial Electrochemistry*, 1983, 147(1-2): 223-234

[17] Wang G, Zhang L, Zhang J. A Review of Electrode Materials for Electrochemical Supercapacitors[J]. *Chemical Society Reviews*, 2012, 41(2): 797-828

[18] Manjuraj T, Krishnamurthy G, Bodke Y D, *et al.* Synthesis, XRD, Thermal, Spectroscopic Studies and Biological Evaluation of Co (II), Ni (II) Cu (II) Metal Complexes Derived from 2-Benzimidazole[J]. *Journal of Molecular Structure*, 2018, 1171: 481-487

[19] Bianchi C, Datta A K, Dughiero F. Mechanistic Understanding of Plasma Arcing in Microwave Food Processing[J]. *Chemical Engineering Science*, 2019, 195: 141-158

[20] Zhang Y, Kang X, Tan J, *et al.* Influence of Calcination and Acidification on Structural Characterization of Anyang Anthracites[J]. *Energy & Fuels*, 2013, 27(11): 7 191-7 197

[21] Chen K, Liu F, Xue D, *et al.* Carbon with Ultrahigh Capacitance when Graphene Paper Meets K 3 Fe (CN) 6[J]. *Nanoscale*, 2015, 7(2): 432-439

[22] Li W, Zhu Y. Structural Characteristics of Coal Vitrinite During Pyrolysis[J]. *Energy & Fuels*, 2014, 28(6): 3 645-3 654

[23] Kaneko K, Ishii C, Rrike M, *et al.* Origin of Superhigh Surface Area and Microcrystalline Graphitic Structures of Activated Carbons[J]. *Carbon*, 1992, 30(7): 1 075-1 088

[24] Menendez J A, Arenillas A, Fidalgo B, *et al.* Microwave Heating Processes Involving Carbon Materials[J]. *Fuel Processing Technology*, 2010, 91(1): 1-8

[25] Ao W, Fu J, Mao X, *et al*. Microwave Assisted Preparation of Activated Carbon from Biomass: A Review[J]. *Renewable and Sustainable Energy Reviews*, 2018, 92: 958-979

[26] Wang Q, Cao Q, Wang X, *et al*. A High-Capacity Carbon Prepared from Renewable Chicken Feather Biopolymer for Supercapacitors[J]. *Journal of Power Sources*, 2013, 225: 101-107

[27] Kopyscinski J, Rahman M, Gupta R, *et al*. K_2CO_3 Catalyzed CO_2 Gasification of Ash-Free Coal. Interactions of the Catalyst with Carbon in N_2 and CO_2 Atmosphere[J]. *Fuel*, 2014, 117(1): 1 181-1 189

[28] He X, Lei J, Geng Y, *et al*. Preparation of Microporous Activated Carbon and Its Electrochemical Performance for Electric Double Layer Capacitor[J]. *Journal of Physics and Chemistry of Solids*, 2009, 70(3-4): 738-744

[29] Xu Z, Yuan Z, Zhang D, *et al.* Highly Mesoporous Activated Carbon Synthesized by Pyrolysis of Waste Polyester Textiles and $MgCl_2$: Physiochemical Characteristics and Pore-Forming Mechanism[J]. *Journal of Cleaner Production*, 2018, 192: 453-461

[30] Guo Y, Shi Z, Chen M, *et al*. Hierarchical Porous Carbon Derived from Sulfonated Pitch for Electrical Double Layer Capacitors[J]. *Journal of Power Sources*, 2014, 252: 235-243

[31] Hastak R S, Sivaraman P, Potphode D D, *et al.* High Temperature All Solid State Supercapacitor Based on Multi-Walled Carbon Nanotubes and Poly [2, 5 Benzimidazole][J]. *Journal of Solid State Electrochemistry*, 2012, 16(10): 3 215-3 226

[32] Gao X, Xing W, Zhou J, *et al*. Superior Capacitive Performance of Active Carbons Derived from Enteromorpha Prolifera[J]. *Electrochimica Acta*, 2014, 133: 459-466

[33] Kim T Y, Jung G, Yoo S, *et al.* Activated Graphene-Based Carbons as Supercapacitor Electrodes with Macro- and Mesopores[J]. *ACS Nano*, 2013, 7(8): 6 899-6 905

[34] You C, Yan X, Kong J, *et al.* Direct Electrochemistry of Myoglobin Based on Bicontinuous Gyroidal Mesoporous Carbon Matrix[J]. *Electrochemistry Communications*, 2008, 10(12): 1 864-1 867